Eur. Phys. J. D (2023) 77:39
https://doi.org/10.1140/epjd/s10053-023-00621-9

THE EUROPEAN PHYSICAL JOURNAL D

Check for updates

Regular Article – Plasma Physics

Higher-order nonlinear dust ion acoustic (DIA) solitary waves in plasmas with weak relativistic effects in electrons and ions

Samiran Das[1,a] and Dulal Chandra Das[2,b]

[1] Department of Mathematics, Central Institute of Technology Kokrajhar, BTR, Kokrajhar, Assam 783370, India
[2] Department of Mathematics, Barnagar College, Sorbhog, Barpeta, Assam 781317, India

Received 2 November 2022 / Accepted 16 February 2023 / Published online 9 March 2023

Abstract. In this new investigation of higher-order nonlinear dust ion acoustic (DIA) waves with negative dust charges and weakly relativistic ions and electrons in the plasma, only compressive DIA solitons of interesting characters are established through the modified Korteweg–de Vries equation which is derived through standard perturbation technique. Important characteristics of amplitudes and width of relativistic DIA solitary waves are investigated in this new investigation for different plasma parameters. It is found that the amplitude of the solitons increases for smaller streaming speed to ions and electrons with the increment of dust-to-ion density ratio, whereas it is opposite for higher streaming speed of ions and electrons. It is also found that the amplitude of the compressive solitons remains unaffected and linearly increases with the enhancement of dust charges in the plasma. Finally, application of this study to astrophysical and space plasma is discussed briefly.

1 Introduction

A macroscopically neutral gas called plasma contains interacting charged particles (ions and electrons) and neutrals occupied 99% of the matter in our universe in which the dust is one of the omnipresent ingredients. These dust particles of different sizes are charged either negatively or positively depending on their surrounding plasma environments [1]. Thus, dusts in the space plasma [2], inter-planetary space, interstellar or molecular clouds, comet tails [1], interstellar medium [3], circumstellar clouds, solar system, planetary rings [4], become one of the major plasma particles along with ions, electrons and neutral particles in determining plasma characteristics. Reception of dust charges by plasma particles affects the growth of amplitudes of compressive solitons [5]. The dust particles in the stationary background [6] also affect the propagation of plasma waves by obstructing the initial streaming speed of ions and electrons, and it sustains [7] even in the case of relativistic electrons. The presence of dust particles in the space plasma as well as laboratory plasma plays very important role in the study of significant characteristics of plasmas, such as the low-frequency electrostatic noise [8] in the region of higher dust particles of Halley's comet, Saturn's F-rings [9], contributions to the mutual interactions [10] between other plasma particles, damping [11,12] in the wave propagation and phase velocity [13], shock waves [14] due to the presence of non-adiabatic dust charges, chaotic behaviors of dust ion acoustic waves in unmagnetized plasma [15] which are few examples among many more. The amount of dust charges in a dust grain is another factor of consideration as it can drastically change the amplitudes of the compressive and rarefactive Korteweg–de Vries (KdV) solitons [16].

Investigation of plasma model with different compositions of plasma particles helps to understand various characteristics and behavior of plasmas. In electronegative dusty plasma with negatively charged dust particles [17,18], the external magnetic field [19,20] and non-thermal negative ions significantly change the speed, amplitude, width of dust ion acoustic solitary waves (DIASWs). Also, positively charged [21] dust species reduces the phase velocity of the ion acoustic (IA) waves and supports IA subsonic compressive solitary waves. In unmagnetized dusty plasma, the vortex-like phase space distribution of ions [22] shows larger amplitude, smaller width but high velocity than that of adiabatic ions.

Plasma composition with relativistic effects on plasma particles adds an advance stage of investigation in the study of plasma behavior. The nature of solitary waves in a fully relativistic plasma [23] from one type to another depends on the density of charged dust particles (negatively charged or positively charged). Relativistic ion density and electron temperature play key

[a] e-mail: s.das@cit.ac.in (corresponding author)
[b] e-mail: ph20maths1002@cit.ac.in

role in the change of amplitudes [24] and propagation of solitary waves. In a plasma consisting of weakly relativistic electrons and ions together with immobile negatively charged dust particles [25], massive ions are predominant and there exists a definite interval for ion streaming speed in which DIA compressive relativistic solitons exist. The amplitude of dust ion acoustic solitary waves decreases with the decrease (or increase) in the streaming speed of relativistic ions [26] in the absence of ion pressure (or presence of ion pressure), respectively. The relativistic effects on trapped electrons using vortex-like distribution restrict the region of existence of solitary waves [27]. Solitary waves are also confirmed by sufficiently available non-thermal ions [28] and negatively charged dust grains. The increment in ion-to-electron ratio [29] and dust charges with both relativistic or non-relativistic ions and electrons reduces the amplitudes of solitary waves.

Two important waves, namely solitary waves [30] and dust acoustic waves [31], in the investigation of dusty plasma can be analyzed through Korteweg–de Vries (KdV) equation and modified Korteweg–de Vries (mKdV) equation, and these equations can be derived by reductive perturbation technique (RPT) [32], in which size of perturbation plays significant role in the connection of initial ion streaming, dust charge number and non-thermal parameter with mKdV solitons [33]. In this paper, we investigated higher-order nonlinear dust-ion acoustic (DIA) waves with negative dust charges and weakly relativistic ions and electrons in the plasma through modified Korteweg–de Vries (mKdV) equation derived by using reductive perturbation technique (RPT). The paper is arranged in sequence: introduction in Sect. 1, governing equations in Sect. 2, derivation of modified Korteweg–de Vries (mKdV) equation in Sect. 3, solution of modified Korteweg–de Vries (mKdV) equation in Sect. 4, results and discussion in Sect. 5 followed by references in the last section.

2 Governing equations

The present plasma model consists of mobile dust particles, weakly relativistic electrons and ions with variable pressure. The nonlinear propagation of dust ion acoustic solitary waves (DIASWs) is governed by equation of continuity and conservation of momentum for dusts and ions supplemented with Poisson's equation as follows:

$$\frac{\partial n_d}{\partial t} + \frac{\partial (n_d u_d)}{\partial x} = 0 \tag{1}$$

$$\frac{\partial u_d}{\partial t} + u_d \frac{\partial u_d}{\partial x} = \frac{\partial \phi}{\partial x} \tag{2}$$

$$\frac{\partial n_i}{\partial t} + \frac{\partial (n_i u_i)}{\partial x} = 0 \tag{3}$$

$$\frac{\partial}{\partial t}(\gamma_i u_i) + u_i \frac{\partial}{\partial x}(\gamma_i u_i) + \frac{\alpha}{n_i}\frac{\partial p_i}{\partial x} = -\frac{\partial \phi}{\partial x} \tag{4}$$

$$\frac{\partial p_i}{\partial t} + u_i \frac{\partial p_i}{\partial x} + 3p_i \frac{\partial}{\partial x}(\gamma_i u_i) = 0 \tag{5}$$

$$\frac{\partial n_e}{\partial t} + \frac{\partial (n_e u_e)}{\partial x} = 0 \tag{6}$$

$$\frac{\partial}{\partial t}(\gamma_e u_e) + u_e \frac{\partial}{\partial x}(\gamma_e u_e) = \frac{1}{Q}\left(\frac{\partial \phi}{\partial x} - \frac{1}{n_e}\frac{\partial n_e}{\partial x}\right) \tag{7}$$

$$\frac{\partial^2 \phi}{\partial x^2} = n_e + Z_d n_d - n_i \tag{8}$$

where u_d, u_i, u_e are velocities and n_d, n_i, n_e are densities of the movable dust particles, ions and electrons, respectively, Z_d is the number of charges contained in a dust grain, ϕ is the velocity potential of the wave, p_i is the pressure of positive ions, $\alpha_i = \frac{T_i}{T_e}$ is the ion-to-electron temperature ratio, $Q = \frac{m_e}{m_i}$ is the electron-to-ion mass ratio, and $\gamma_i = \left(1 - \frac{u_i^2}{c^2}\right)^{-\frac{1}{2}}, \gamma_e = \left(1 - \frac{u_e^2}{c^2}\right)^{-\frac{1}{2}}$.

The flow variables are normalized by following the usual procedure of normalization [28] as: The densities are normalized by the respective equilibrium ion density n_{i0}, space by the electron Debye length λ_{De}, time by the inverse of the ion plasma frequency $\omega_{pi}^{-1} = \left(\frac{4\pi n_0 e^2}{m_i}\right)^{-1/2}$, velocities by $c_s = \left(\frac{KT_e}{m_i}\right)^{1/2}$, pressure by equilibrium plasma pressure $p_{i0} = n_{i0}KT_i, p_{e0} = n_{e0}KT_e$ and potential ϕ by $\frac{KT_e}{e}$.

3 Derivation of modified Korteweg–de Vries (mKdV) equation

Using the stretched variables

$$\xi = \varepsilon^{1/2}(x - Vt), \qquad \tau = \varepsilon^{3/2}Vt \tag{9}$$

(where V is the phase velocity of waves), the Korteweg–de Vries (KdV) equation was derived [5] from the set of equations (1 - 8) as

$$\frac{\partial \phi_1}{\partial \tau} + p'\phi_1\frac{\partial \phi_1}{\partial \xi} + q'\frac{\partial^3 \phi_1}{\partial \xi^3} = 0 \tag{10}$$

where $p' = AB, q' = -A$ with

$$A=\frac{(u_{d0}-V)^3\{(u_{i0}-V)^2-3\alpha\}^2\left(1+\frac{3u_{i0}^2}{2c^2}\right)\{Q(u_{e0}-V)^2\left(1+\frac{3u_{e0}^2}{2c^2}\right)-1\}^2}{\begin{array}{l}2V\sigma Z_d\{(u_{i0}-V)^2-3\alpha\}^2\left(1+\frac{3u_{i0}^2}{2c^2}\right)\{Q(u_{e0}-V)^2\left(1+\frac{3u_{e0}^2}{2c^2}\right)-1\}^2\\ \quad+2V(u_{i0}-V)(u_{d0}-V)^3\{Q(u_{e0}-V)^2\left(1+\frac{3u_{e0}^2}{2c^2}\right)-1\}^2\\ \quad+2VQ(1-\sigma Z_d)(u_{e0}-V)\left(1+\frac{3u_{e0}^2}{2c^2}\right)(u_{d0}-V)^3\{(u_{i0}-V)^2-3\alpha\}^2\left(1+\frac{3u_{i0}^2}{2c^2}\right)\end{array}}$$

$$B=\frac{2Q(1-\sigma Z_d)(u_{e0}-V)^2\left(1+\frac{3u_{e0}^2}{2c^2}\right)}{\begin{array}{l}\{Q(u_{e0}-V)^2\left(1+\frac{3u_{e0}^2}{2c^2}\right)-1\}^3+\frac{3Qu_{e0}(1-\sigma Z_d)(u_{e0}-V)^3}{c^2\{Q(u_{e0}-V)^2\left(1+\frac{3u_{e0}^2}{2c^2}\right)-1\}^3}\\ \quad+\frac{1-\sigma Z_d}{\{Q(u_{e0}-V)^2\left(1+\frac{3u_{e0}^2}{2c^2}\right)-1\}^2}+\frac{3\sigma Z_d}{(u_{d0}-V)^4}-\frac{3}{\{(u_{i0}-V)^2-3\alpha\}^2\left(1+\frac{3u_{i0}^2}{2c^2}\right)^2}-\frac{3\alpha}{\{(u_{i0}-V)^2-3\alpha\}^3\left(1+\frac{3u_{i0}^2}{2c^2}\right)^2}\\ \quad-\frac{3u_{i0}(u_{i0}-V)}{c^2\{(u_{i0}-V)^2-3\alpha\}^2\left(1+\frac{3u_{i0}^2}{2c^2}\right)^3}-\frac{9\alpha}{\{(u_{i0}-V)^2-3\alpha\}^3\left(1+\frac{3u_{i0}^2}{2c^2}\right)^2}\end{array}}$$

For a multi-species plasma, there is a density regime (called critical density) where B vanishes. As the nonlinear term in (10) disappears, the stretching (9) invalids and a different stretching to enter into higher-order nonlinearity is needed.

Hence, for higher-order nonlinearity and to derive the mKdV equation, we use the following (11) stretched variables [34–37], determined from corresponding dispersion relation of the set of equations (1 - 8)

$$\xi=\varepsilon(x-Vt),\qquad \tau=\varepsilon^3Vt \tag{11}$$

with the phase velocity V of the waves. The expressions of the flow variables in terms of the small parameter ε are taken as:

$$\left.\begin{array}{l}n_d=n_{d0}+\varepsilon n_{d1}+\varepsilon^2n_{d2}+\dots\\ u_d=u_{d0}+\varepsilon u_{d1}+\varepsilon^2u_{d2}+\dots\\ n_i=n_{i0}+\varepsilon n_{i1}+\varepsilon^2n_{i2}+\dots\\ u_i=u_{i0}+\varepsilon u_{i1}+\varepsilon^2u_{i2}+\dots\\ n_e=n_{e0}+\varepsilon n_{e1}+\varepsilon^2n_{e2}+\dots\\ u_e=u_{e0}+\varepsilon u_{e1}+\varepsilon^2u_{e2}+\dots\\ p_i=p_{i0}+\varepsilon p_{i1}+\varepsilon^2p_{i2}+\dots\\ \phi=\varepsilon\phi_1+\varepsilon^2\phi_2+\dots\end{array}\right\} \tag{12}$$

Following the standard perturbation technique, with the use of transformations (11) and expansions (12) in the normalized set of equations (1 - 8), using the boundary conditions,$n_{d1}=0,u_{d1}=0,n_{i1}=0,u_{i1}=0,n_{e1}=0,u_{e1}=0,p_{i1}=0,\phi_1=0$, as $|\xi|\to\infty$, in the first-order equations in ε after integration, we get first-order quantities as

$$\begin{aligned}&u_{d1}=\frac{\phi_1}{B_d},\quad n_{d1}=\frac{-n_{d0}\phi_1}{B_d^2},\quad u_{i1}=\frac{-B_i\phi_1}{E_i\left(B_i^2-3\alpha\right)},\\ &n_{i1}=\frac{n_{i0}\phi_1}{E_i\left(B_i^2-3\alpha\right)},\quad u_{e1}=\frac{B_e\phi_1}{-1+QE_eB_e^2},\\ &n_{e1}=\frac{-n_{e0}\phi_1}{-1+QE_eB_e^2},\quad p_{i1}=\frac{3p_{i0}\phi_1}{B_i^2-3\alpha}\end{aligned} \tag{13}$$

where, $E_i=1+\frac{3u_{i0}^2}{2c^2}+\frac{15u_{i0}^4}{8c^4}, E_e=1+\frac{3u_{e0}^2}{2c^2}+\frac{15u_{e0}^4}{8c^4}, B_i=u_{i0}-V, B_e=u_{e0}-V$ and $\frac{p_{i0}}{n_{i0}}=1$.

The zero-order equation from the Poisson's equation (8) gives

$$\begin{aligned}&n_{e0}+Z_dn_{d0}-n_{i0}=0\implies\frac{n_{e0}}{n_{i0}}=1-\sigma Z_d,\quad\text{where}\\ &\sigma=\frac{n_{d0}}{n_{i0}},\text{dust-to-ion density ratio}\end{aligned} \tag{14}$$

and by putting the values of first-order perturbed quantities from (13) into the Poisson's first-order equation $n_{e1}-n_{i1}+Z_dn_{d1}=0$ and using (14), we obtain the phase velocity equation as

$$\frac{1-\sigma Z_d}{-1+QE_eB_e^2}+\frac{1}{E_i\left(B_i^2-3\alpha\right)}+\frac{\sigma Z_d}{B_d^2}=0 \tag{15}$$

Again, by using the boundary conditions, $n_{d2}=0,u_{d2}=0,n_{i2}=0,u_{i2}=0,n_{e2}=0,u_{e2}=0,p_{i2}=0,\phi_2=0$, as $|\xi|\to\infty$, in the second-order equations in ε after integration, we get second-order perturbed quantities as

$$\left.\begin{array}{l} n_{d2}=\frac{3n_{d0}}{2B_d^4}\phi_1^2-\frac{n_{d0}}{B_d^2}\phi_2, \quad u_{d2}=\frac{-1}{2B_d^3}\phi_1^2+\frac{1}{B_d}\phi_2,\\ n_{i2}=n_{i0}R\phi_1^2+n_{i0}\frac{1}{E_iL}\phi_2,\ u_{i2}=-S\phi_1^2-\frac{B_i}{E_iL}\phi_2,\\ p_{i2}=p_{i0}R_1\phi_1^2+p_{i0}\frac{3}{L}\phi_2, \quad n_{e2}=n_{e0}S_1\phi_1^2-n_{e0}\frac{1}{M}\phi_2,\\ u_{e2}=-M_1\phi_1^2+\frac{B_e}{M}\phi_2 \end{array}\right\} \tag{16}$$

where

$$L=B_i^2-3\alpha, \quad M=-1+QE_eB_e^2,$$
$$F_i=\frac{12c^2u_{i0}+30u_{i0}^3}{8c^4},$$
$$F_e=\frac{12c^2u_{e0}+30u_{e0}^3}{8c^4}$$
$$R=\frac{E_i\,(2L-3\alpha+9E_i\alpha)-6F_i\alpha B_i+3E_iB_i^2+2F_iB_i^3}{2E_i^3L^3},$$
$$S=\frac{B_i\Big(E_i\,(2L+3\alpha+9E_i\alpha)-6F_iB_i\alpha+E_iB_i^2+2F_iB_i^3\Big)}{2E_i^3L^3}$$
$$R_1=\frac{3\Big(2L+(2+3E_i)B_i^2\Big)}{2E_iL^3},$$
$$S_1=\frac{2M+(3E_e+2B_eF_e)QB_e^2}{2M^3},$$
$$M_1=\frac{B_e\Big(2(1+M)+(E_e+2B_eF_e)QB_e^2\Big)}{2M^3}$$

Further (14) and (16) together with Poisson's second-order equation $n_{e2}-n_{i2}+Z_dn_{d2}=0$ give

$$2B_d^4\Big(R+(1-\sigma Z_d)S_1\Big)-3\sigma Z_d=0 \tag{17}$$

From Poisson's third-order equation $\frac{\partial^2\phi_1}{\partial\xi^2}=n_{e3}-n_{i3}+Z_dn_{d3}$, we get

$$\frac{\partial^3\phi_1}{\partial\xi^3}=\frac{\partial n_{e3}}{\partial\xi}-\frac{\partial n_{i3}}{\partial\xi}+Z_d\frac{\partial n_{d3}}{\partial\xi} \tag{18}$$

From third-order equations in ε, we get

$$\left.\begin{array}{l} B_d\frac{\partial n_{d3}}{\partial\xi}+\frac{\partial}{\partial\xi}\Big(n_{d2}u_{d1}+n_{d1}u_{d2}\Big)+n_{d0}\frac{\partial u_{d3}}{\partial\xi}+V\frac{\partial n_{d1}}{\partial\tau}=0\\ B_d\frac{\partial u_{d3}}{\partial\xi}+\frac{\partial}{\partial\xi}\Big(u_{d1}u_{d2}\Big)+V\frac{\partial u_{d1}}{\partial\tau}-\frac{\partial\phi_3}{\partial\xi}=0\\ B_i\frac{\partial n_{i3}}{\partial\xi}+\frac{\partial}{\partial\xi}\Big(n_{i2}u_{i1}+n_{i1}u_{i2}\Big)+n_{i0}\frac{\partial u_{i3}}{\partial\xi}+V\frac{\partial n_{i1}}{\partial\tau}=0\\ B_in_{i0}E_i\frac{\partial u_{i3}}{\partial\xi}+\alpha\frac{\partial p_{i3}}{\partial\xi}+\Big(F_iB_i+E_i\Big)n_{i1}\frac{\partial(u_{i1}^2)}{\partial\xi}\\ \quad+2\Big(F_iB_i+E_i\Big)n_{i0}\frac{\partial(u_{i1}u_{i2})}{\partial\xi}+B_iE_i\frac{\partial}{\partial\xi}\\ \times\Big(n_{i1}u_{i2}+n_{i2}u_{i1}\Big)+2n_{i0}G_i\frac{\partial(u_{i1}^3)}{\partial\xi}+Vn_{i0}E_i\frac{\partial u_{i1}}{\partial\tau}\\ +n_{i2}\frac{\partial\phi_1}{\partial\xi}+n_{i1}\frac{\partial\phi_2}{\partial\xi}+n_{i0}\frac{\partial\phi_3}{\partial\xi}=0\\ B_i\frac{\partial p_{i3}}{\partial\xi}+3p_{i0}E_i\frac{\partial u_{i3}}{\partial\xi}+3F_ip_{i1}\frac{\partial(u_{i1}^2)}{\partial\xi}\\ +(1+3E_i)\frac{\partial}{\partial xi}\Big(p_{i2}u_{i1}+u_{i2}p_{i1}\Big)+p_{i0}H_i\frac{\partial(u_{i1}^3)}{\partial\xi}\\ +36p_{i0}u_{i0}(2c^2+5u_{i0}^2)\frac{\partial}{\partial\xi}(u_{i1}u_{i2})+V\frac{\partial p_{i1}}{\partial\tau}=0\\ B_e\frac{\partial n_{e3}}{\partial\xi}+\frac{\partial}{\partial\xi}\Big(n_{e2}u_{e1}+n_{e1}u_{e2}\Big)+n_{e0}\frac{\partial u_{e3}}{\partial\xi}\\ +V\frac{\partial n_{e1}}{\partial\tau}=0QB_en_{e0}E_e\frac{\partial u_{e3}}{\partial\xi}\\ +\frac{\partial n_{e3}}{\partial\xi}+\Big(F_eB_e+E_e\Big)n_{e1}\frac{\partial(u_{e1}^2)}{\partial\xi}\\ +2Qn_{e0}\Big(F_eB_e+E_e\Big)\frac{\partial(u_{e1}u_{e2})}{\partial\xi}\\ +B_eE_e\frac{\partial}{\partial\xi}\Big(n_{e1}u_{e2}+n_{e2}u_{e1}\Big)\\ +2Qn_{e0}G_e\frac{\partial(u_{e1}^3)}{\partial\xi}+QVn_{e0}E_e\frac{\partial u_{e1}}{\partial\tau}-n_{e2}\frac{\partial\phi_1}{\partial\xi}\\ -n_{e1}\frac{\partial\phi_2}{\partial\xi}-n_{e0}\frac{\partial\phi_3}{\partial\xi}=0 \end{array}\right\} \tag{19}$$

Solving for $\frac{\partial n_{d3}}{\partial\xi}$, $\frac{\partial n_{i3}}{\partial\xi}$, $\frac{\partial n_{e3}}{\partial\xi}$ from equation (19) and by substituting in (18), with results from (13 - 17), we found the modified Korteweg–de Vries (mKdV) equation as

$$\frac{\partial\phi_1}{\partial\tau}+p\phi_1^2\frac{\partial\phi_1}{\partial\xi}+q\frac{\partial^3\phi_1}{\partial\xi^3}=0 \tag{20}$$

where, $p=\frac{X}{Y}$, $\quad q=\frac{-1}{Y}$ and

$$X=\Bigg(-\frac{R}{E_iL}-\frac{6SB_i}{E_iL^2}-\frac{2B_i^2}{E_i^3L^4}-\frac{6F_iSB_i^2}{E_i^2L^2}$$
$$-\frac{2F_iB_i^3}{E_i^4L^4}+\frac{6G_iB_i^3}{E_i^4L^4}\Bigg)$$
$$+(1-\sigma Z_d)\Bigg(-\frac{2E_eB_e^2}{M^4}-\frac{2F_eB_e^3}{M^4}$$

$$+\frac{6G_eQB_e^3}{M^4}+\frac{3E_eB_eM_1}{M^2}-\frac{9E_eQB_eM_1}{M^2}-\frac{6F_eQB_e^2M_1}{M^2}+\frac{S_1}{M}-\frac{3E_eB_e^2S_1}{M^2}+\frac{3E_eQB_e^2S_1}{M^2}\Bigg)+\left(\frac{9R\alpha}{E_iL^2}-\frac{27S\alpha}{L^2B_i}+\frac{18F_i\alpha B_i}{E_i^3L^4}-\frac{3H_i\alpha B_i^2}{E_i^4L^4}-\frac{3\alpha R_1}{E_i^2L^2}-\frac{9\alpha R_1}{E_iL^2}+\frac{216c^2S\alpha u_{i0}}{E_i^2L^2}+\frac{540S\alpha u_{i0}^3}{E_i^2L^2}\right)-\frac{15\sigma Z_d}{2B_d^6},$$

$$Y=n_{i0}\left((1-\sigma Z_d)\left(\frac{2E_eQVB_e}{M^2}-\frac{\alpha V}{E_iLMB_i}\right)+\frac{2B_iV}{E_iL^2}-\frac{3\alpha V}{E_iL^2B_i}+\frac{2\sigma Z_dV}{B_d^3}\right),$$

$$G_i=-2c^2V+8c^2u_{i0}-15Vu_{i0}^2+30u_{i0}^3,$$
$$G_e=-2c^2V+8c^2u_{e0}-15Vu_{e0}^2+30u_{e0}^3,$$
$$H_i=12c^2+90u_{i0}^2.$$

4 Solution of modified Korteweg–de Vries (mKdV) equation

The solution of mKdV equation (20) is obtained by substituting $\eta=\xi-C_1\tau$, (C_1 is speed of the soliton) and imposing boundary conditions $\phi_1=\frac{d^2\phi_1}{d\eta^2}=\frac{d\phi_1}{d\eta}=0$ as $|\eta|\to\infty$ as

$$\phi_1=\phi_0\,\mathrm{sech}\left(\frac{\eta}{\Delta}\right)$$

The amplitude of the soliton is $\phi_0=\sqrt{\frac{6C_1}{p}}$, and $\Delta=\sqrt{\frac{q}{C_1}}$ is the width of the wave.

5 Results and discussion

For the complex plasma model with relativistic electrons and ions, only compressive dust ion acoustic modified Korteweg–de Vries (DIA-mKdV) solitons of interesting characters are found to exist.

The amplitudes of compressive modified KdV (Korteweg–de Vries) relativistic solitons for very small $u_{d0}=1$ starting with reasonable amplitude sharply increase convexly and then increase linearly (remaining constant) to a certain range ($u_{e0}\approx 12-36$) and thereafter decrease concavely to vanish at very high initial streaming of electrons ($u_{e0}>60$), for other values of parameters, dust-to-ion density ratio ($\sigma=0.0001$), ion-to-electron temperature ratio ($\alpha=0.1$), $u_{i0}=30$, and dust charges ($Z_d=200(i),600(ii),1000(iii)$) (Fig. 1a). The growth of amplitudes of the relativistic mKdV solitons becomes more sharp as the number of charges contained in a dust particle increases ($Z_d=200-1000$), remaining other parameters same in all the three cases $Z_d=200(i),600(ii),1000(iii)$. Also, the region of flatness ($14<u_{i0}<37$) increases with the increase in dust charges. The growth pattern of relativistic mKdV solitons is reflected in Fig. 1a, clearly showing the variations of amplitudes of solitons on u_{e0}. Figure 1b shows amplitudes (ϕ_0) of compressive relativistic mKdV solitary waves versus initial ion streaming u_{i0}. Amplitudes of relativistic dust-ion acoustic (DIA) mKdV solitons remain constant for $u_{i0}<14$ and for $\sigma=0.0001,\alpha=0.1,u_{d0}=1,u_{e0}=20,Z_d=200(i),600(ii)$ and $1000(iii)$. The amplitudes of compressive DIA-mKdV solitons increase convexly very sharply in a very short range of u_{i0} for all the values of $Z_d=200(i),600(ii)$ and $1000(iii)$. As number of dust charges increase, amplitudes of compressive DIA-mKdV solitons decrease (Fig. 1a), showing the same characteristic growth for all the values of Z_d with other parametric values same as above. Figure 1d, e depicts the clear view of amplitudes in three dimensions for the same values of parameters as in Fig. 1a, b, respectively. It is noteworthy to mention that for smaller and equal initial streamings of relativistic ions and electrons, viz. $u_{i0}=u_{e0}=10$, amplitudes of the compressive DIA-mKdV solitons remain constant for $u_{d0}\le 12$, thereafter increases sharply in a very smaller range of u_{d0} and then again decreases with the increase of u_{d0} for $\sigma=0.0001,\alpha=0.1,Z_d=200(i),600(ii),1000(iii)$ (Fig. 1c). It is interesting to observe that for this case (lower and equal values of relativistic ions and electrons), the compressive DIA-mKdV solitons exist for $u_{d0}<40$ (Fig. 1c, f). Hence, existence range of compressive DIA-mKdV solitons increases with the increase in initial streamings of relativistic ions and electrons (Fig. 1a–c) keeping the smaller values of initial streaming of heavier dust particles which is a salient feature of this investigation.

The compressive DIA-mKdV solitons are found to exist for equal and large values of initial streaming speeds of ions and electrons, viz. $u_{i0}=50=u_{e0}$, and for very small initial streaming speed of dust $u_{d0}=5$ with other parametric values as $\sigma=0.0001,\alpha=0.1(i),0.3(ii)$ and $0.5(iii)$. The amplitudes of compressive DIA-mKdV solitons increase linearly (almost constant) with the increase of Z_d (Fig. 2a) with other parametric values as same as above without altering the shape of amplitudes. Higher values of the temperature ratio ($\alpha=0.1(i),0.3(ii),0.5(iii)$) produce compressive DIA-mKdV solitons of higher amplitudes (Fig. 2a, b) maintaining the same shape. Interestingly, for smaller values of the initial streamings of ions and electrons, i.e., $u_{i0}=10,u_{e0}=20$ keeping u_{d0} same as Fig. 2a, compressive DIA-mKdV solitons of same shape and same characteristics are seen to be produced but much smaller amplitudes than that of Fig. 2a (with other parameters also same as for Fig. 2a). So, from Fig. 2a, b, it is clear that higher initial streaming speeds of relativistic electrons and ions produce compressive DIA-mKdV solitons of higher amplitudes. Figure 2c, d shows the pictorial 3D view of Fig. 2a, b, respectively.

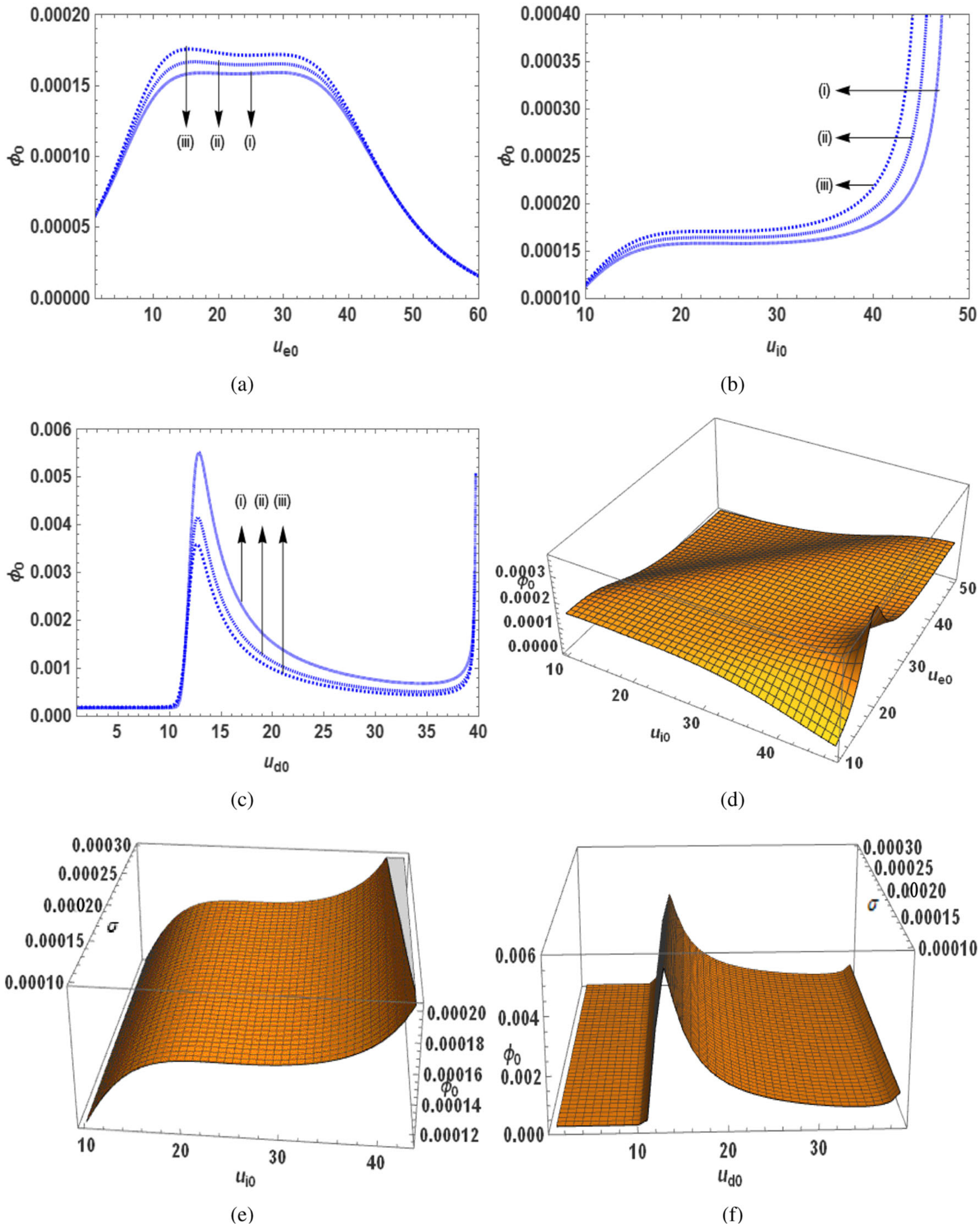

Fig. 1 Amplitudes of compressive mKdV solitons versus (**a**) electrons' streaming speed u_{e0} for fixed $Q = 0.00054, c = 300, \sigma = 0.0001, \alpha = 0.1, u_{i0} = 30, u_{d0} = 1, Z_d = 200(i), 600(ii), 1000(iii)$, (**b**) ions' streaming speed u_{i0} for fixed $u_{d0} = 1, u_{e0} = 20, Q = 0.00054, c = 300, \sigma = 0.0001, \alpha = 0.1, Z_d = 200(i), 600(ii), 1000(iii)$, (**c**) dusts' streaming speed u_{d0} for fixed $u_{i0} = 10, u_{e0} = 10, Q = 0.00054, c = 300, \sigma = 0.0001, \alpha = 0.1, Z_d = 200(i), 600(ii), 1000(iii)$, (**d**) electrons' and ions' streaming speed for fixed $Q = 0.00054, c = 300, \sigma = 0.0001, \alpha = 0.1, u_{d0} = 1, Z_d = 200$, (**e**) ions' streaming speed for fixed $Q = 0.00054, c = 300, u_{e0} = 20, \alpha = 0.1, u_{d0} = 1, Z_d = 200$, (**f**) dusts' streaming speed for fixed $Q = 0.00054, c = 300, u_{e0} = 10, \alpha = 0.1, u_{i0} = 10, Z_d = 200$

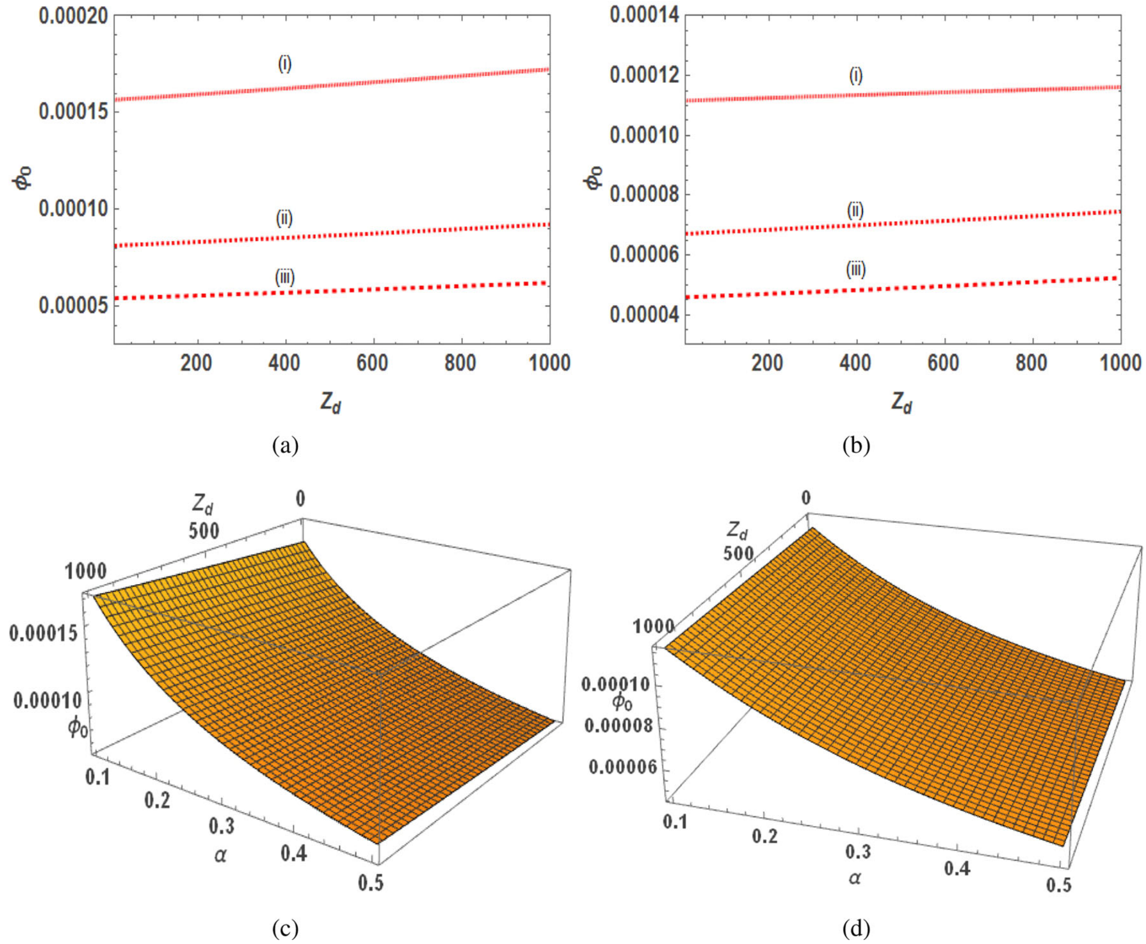

Fig. 2 Amplitudes of compressive mKdV solitons versus dust charges Z_d for fixed (**a**) $Q = 0.00054, c = 300, \sigma = 0.0001, u_{d0} = 5, u_{i0} = 50, u_{e0} = 50, \alpha = 0.1(i), 0.3(ii), 0.5(iii)$, (**b**) $Q = 0.00054, c = 300, \sigma = 0.0001, u_{d0} = 5, u_{i0} = 10, u_{e0} = 20, \alpha = 0.1(i), 0.3(ii), 0.5(iii)$, (c)$Q = 0.00054, c = 300, \sigma = 0.0001, u_{i0} = 50, u_{e0} = 50, u_{d0} = 5$, (d) $Q = 0.00054, c = 300, \sigma = 0.0001, u_{i0} = 10, u_{e0} = 20, u_{d0} = 5$

For smaller values of number of dust charges ($Z_d = 200$), very small-amplitude mKdV compressive solitons are found to remain almost constant (negligible decrease) throughout the range of dust-to-ion density ratio ($\sigma = 0.0001$ to 0.0003) and for higher initial streaming speed of ions ($u_{i0} = 30$), electrons ($u_{e0} = 50$) and lower initial streaming speed of dusts ($u_{d0} = 5$) with $\alpha = 0.1$. It is interesting to observe that as Z_d increases ($Z_d = 600(ii)$), the amplitudes of compressive DIA-mKdV solitons (starting with a reasonable amplitude) start decreasing as σ increases and for very high dust charge ($Z_d = 1000(iii)$) the amplitude decreases suddenly as σ increases, keeping the other parametric values same as above (Fig. 3a). On the other hand, for small value of the initial streaming speed of ions and electrons ($u_{i0} = 10, u_{e0} = 15$), the amplitudes of compressive DIA-mKdV solitons show quite opposite character. For smaller number of dust charges ($Z_d = 200(i)$), the amplitudes increase very slowly (almost linearly) with the increase of $\sigma(= 0.0001$ to $0.0003)$ and for $\alpha = 0.1$ (Fig. 3b). With the increase in the number of charges contained in a dust particle ($Z_d = 600(ii), 1000(iii)$), the amplitudes of DIA solitons increase very fast with the increase of σ and other values of parameters as $u_{i0} = 10, u_{e0} = 15, \alpha = 0.1, u_{d0} = 5$. Hence due to relativistic effect in electrons and ions, the higher values of initial streamings of ions and electrons corresponding amplitudes show decreasing character (Fig. 3a), while for the smaller values, the amplitudes show the opposite character (Fig. 3b) for the same (smaller) values of initial streaming of dust ($u_{d0} = 5$) for both the cases (Fig. 3a, b). Figure 3c, d gives clear picture of the characteristics of amplitudes of DIA solitons.

Amplitude of compressive DIA-mKdV solitons decreases sharply as α increases for $\sigma = 0.0001, u_{d0} = 5, u_{i0} = 50, u_{e0} = 55, Z_d = 200(i), 600(ii), 1000(iii)$. Characteristic change of amplitudes of DIA-mKdV solitons for all the three values of $Z_d = 200(i), 600(ii), 1000(iii)$ remains same as shown in Fig. 4a, b. Higher the initial streaming speeds of relativistic ions and electrons ($u_{i0} = 50, u_{e0} = 55$), higher the amplitudes (Fig. 4a) and for the smaller initial streaming speeds of relativistic ions and electrons ($u_{i0} = 10, u_{e0} = 15$), the smaller the amplitudes of the

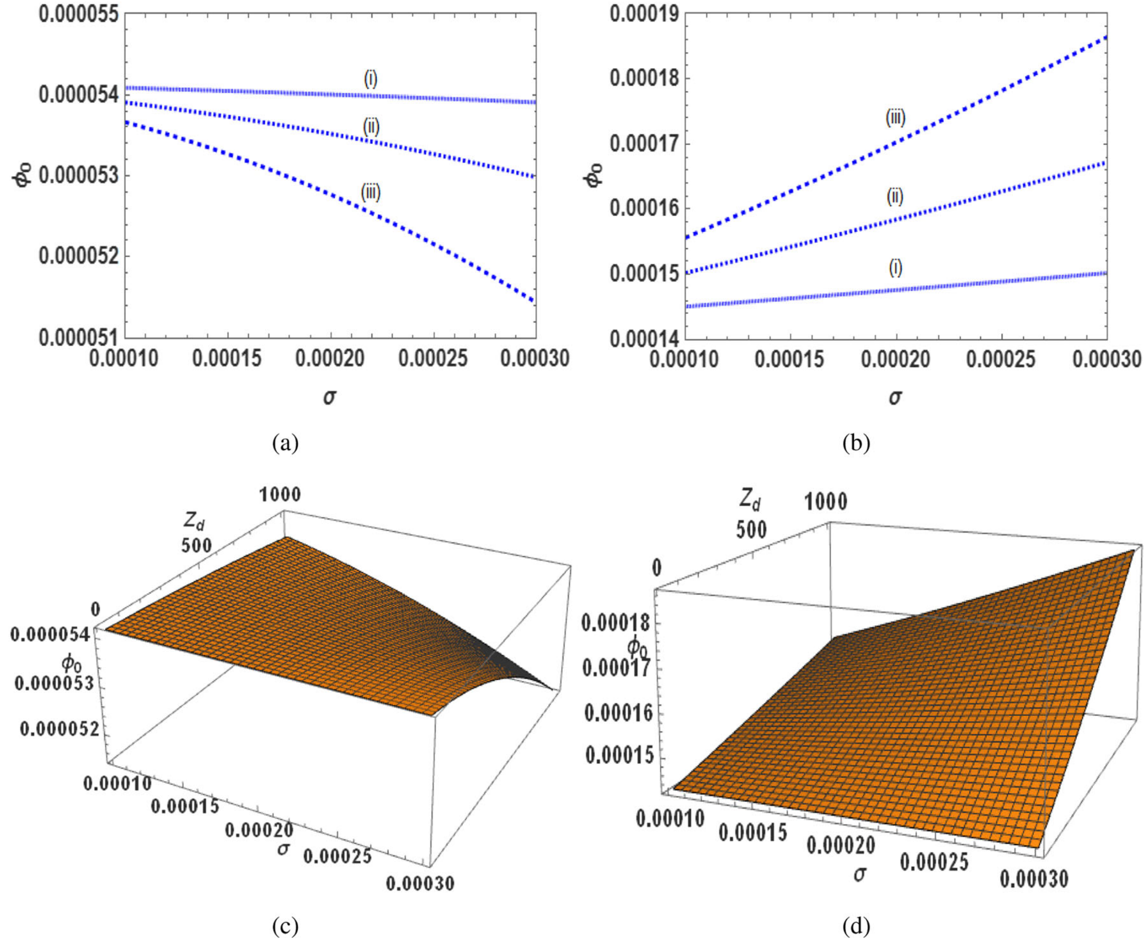

Fig. 3 Amplitudes of compressive mKdV solitons versus dust-to-ion density ratio σ for fixed (**a**) $Q = 0.00054, c = 300, \alpha = 0.1, u_{d0} = 5, u_{i0} = 30, u_{e0} = 50, Z_d = 200(i), 600(ii), 1000(iii)$, (**b**) $Q = 0.00054, c = 300, \alpha = 0.1, u_{d0} = 5, u_{i0} = 10, u_{e0} = 15, Z_d = 200(i), 600(ii), 1000(iii)$, (**c**) $Q = 0.00054, c = 300, \alpha = 0.1, u_{i0} = 30, u_{e0} = 50, u_{d0} = 5$, (**d**) $Q = 0.00054, c = 300, \alpha = 0.1, u_{i0} = 10, u_{e0} = 15, u_{d0} = 5$

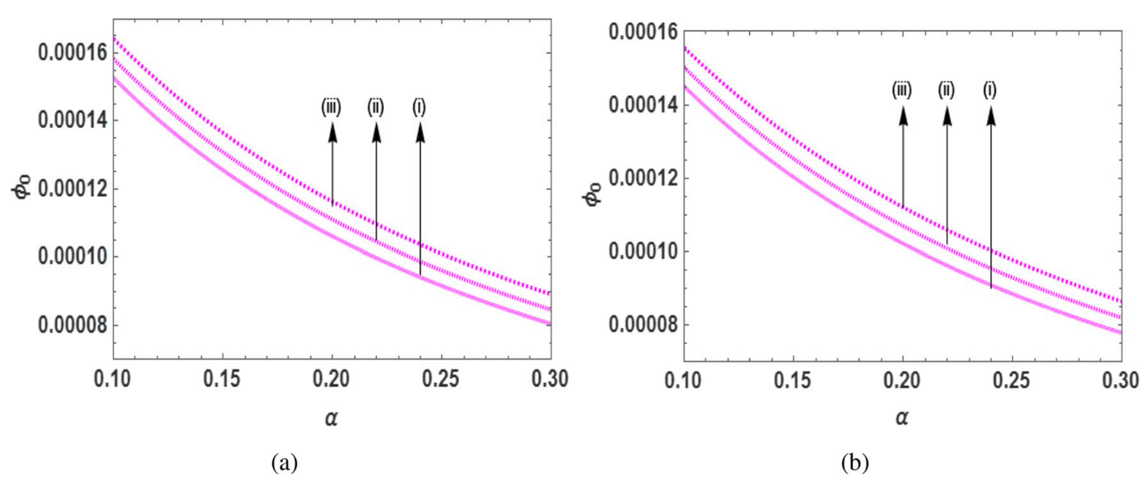

Fig. 4 Amplitudes of compressive mKdV solitons versus ion-to-electron temperature ratio α for fixed **a** $Q = 0.00054, c = 300, \sigma = 0.0001, u_{d0} = 5, u_{i0} = 50, u_{e0} = 55, Z_d = 200(i), 600(ii), 1000(iii)$, **b** $Q = 0.00054, c = 300, \sigma = 0.0001, u_{d0} = 5, u_{i0} = 10, u_{e0} = 15, Z_d = 200(i), 600(ii), 1000(iii)$

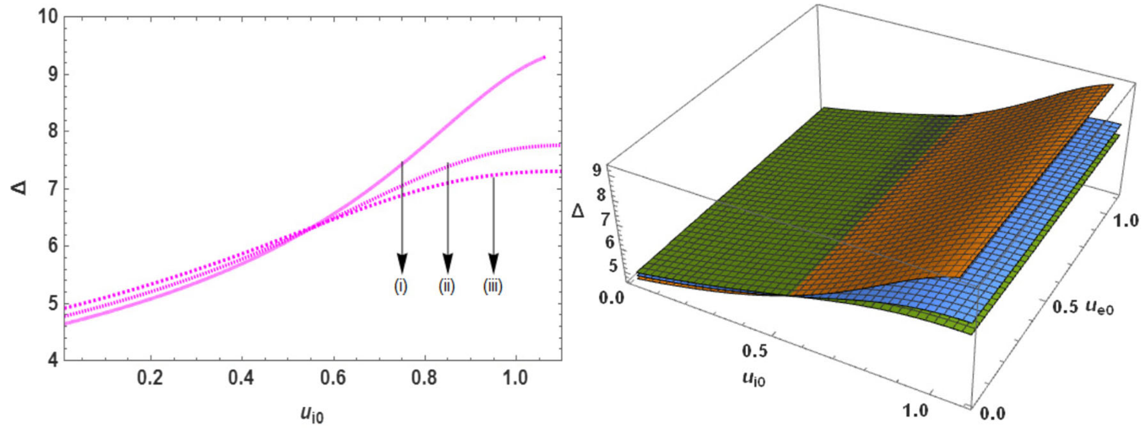

(a) (b)

Fig. 5 Width of compressive mKdV solitons versus ions' streaming speed u_{i0} for fixed $Q = 0.00054, c = 300, \sigma = 0.0001, u_{d0} = 0.1, u_{e0} = 0.1, Z_d = 200(i), 600(ii), 1000(iii)$

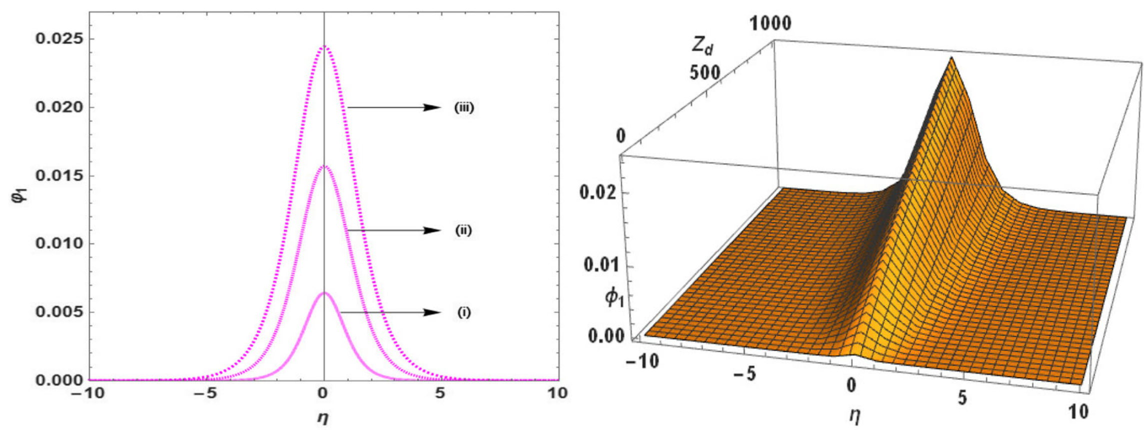

(a) (b)

Fig. 6 Compressive mKdV soliton profiles with respect to space η for three values of dust charges $Z_d = 200(i), 600(ii), 1000(iii)$ and fixed $Q = 0.00054, c = 300, \sigma = 0.0001, \alpha = 0.1, u_{i0} = 30, u_{d0} = 1, u_{e0} = 30$

compressive DIA-mKdV solitons (Fig. 4b) although the difference of the corresponding amplitudes is negligible.

The width of the relativistic compressive DIA-mKdV solitons (corresponding to the amplitudes of solitons in Fig. 5a) becomes great, i.e., the solitary waves become flat (Fig. 5b) for higher number of dust charges ($Z_d = 600(ii), 1000(iii)$) with the increase in initial streaming speed of ions and other parameters as $\sigma = 0.0001, \alpha = 0.1, u_{d0} = 0.1, u_{e0} = 0.1$. The shape of the widths of mKdV compressive solitons (i.e., flatness of the solitary wave) is nicely depicted in Fig. 5b.

The soliton profiles of relativistic compressive mKdV solitons are shown in Fig. 6a, b for $Z_d = 200(i), 600(ii), 1000(iii)$. High-amplitude compressive DIA-mKdV is generated for the higher values of Z_d.

Space probes investigate the properties of dusts present in surroundings of space bodies like the Moon or Mars. Due to the temperature variations to the plasma species, the behavioral changes of the dusts in the DIA waves occur. Our present investigation may be helpful to know the character of the dusts in space probes. The proposed results of our present study of the different plasma parameters may be great help for experimentalists in using the Q-machine.

Author contributions

Both the authors contributed equally in the preparation of this manuscript.

Data Availability Statement This manuscript has no associated data or the data will not be deposited. [Authors' comment: The data that support the findings of this study are available within the article.]

References

1. P.K. Shukla, A.A. Mamun, *Introduction to Dusty Plasma Physics* (IOP Publishing Ltd., 2002)
2. A.A. Mamun, P.K. Shukla, Discoveries of waves in dusty plasmas. J. Plasma Phys. **77**(4), 437–455 (2011)
3. M. Taherimoghadam, I. Motie, A. Bakhshayeshi, T. Mirzaye, Relativistic effects on dust grain charging in

non-equilibrium dusty plasma with relativistic Tsallis distribution. Phys. Plasmas **26**(11), 113704 (2019)
4. A.A. Mamun, The new physics of dust in plasmas. J. Phys.: Conf. Ser. **1718**(1), 012004 (2021)
5. B.C. Kalita, S. Das, Dust ion acoustic (DIA) solitary waves in plasmas with weak relativistic effects in electrons and ions. Astrophys. Space Sci. **352**(2), 585–592 (2014)
6. B.C. Kalita, S. Das, Comparative study of dust ion acoustic Korteweg-de Vries and modified Korteweg-de Vries solitons in dusty plasmas with variable temperatures. J. Plasma Phys. **83**(5), 905830502 (2017)
7. S. Das, Weak Relativistic Effect in the Formation of Ion-Acoustic Solitary Waves in Dusty Plasma. IEEE Trans. Plasma Sci. **50**(7), 2225–2229 (2022)
8. U. De Angelis, V. Formisano, M. Giordano, Ion plasma waves in dusty plasmas: Halley's comet. J. Plasma Phys. **40**(3), 399–406 (1988)
9. P.K. Shukla, V.P. Silin, Dust ion-acoustic wave. Phys. Scr. **45**(5), 508 (1992)
10. P.V. Bliokh, V.V. Yaroshenko, Electrostatic waves in Saturn's rings. Sov. Astron. **29**(3), 330–336 (1985)
11. N. D'Angelo, Ion-acoustic waves in dusty plasmas. Planet. Space Sci. **42**(6), 507–511 (1994)
12. J. Tamang, A. Saha, Influence of dust-neutral collisional frequency and nonextensivity on dynamic motion of dust-acoustic waves. Waves Random Complex Med. **31**(4), 597–617 (2021)
13. Y. Nakamura, H. Bailung, P.K. Shukla, Observation of Ion-Acoustic Shocks in a Dusty Plasma. Phys. Rev. Lett. **83**(8), 1602–1605 (1999)
14. S. Ghosh, S. Sarkar, M. Khan, M.R. Gupta, Dust ion acoustic shock waves in a collisionless dusty plasma. Phys. Lett. A **274**, 162–169 (2000)
15. A. Saha, P. Chatterjee, Solitonic, periodic, quasiperiodic and chaotic structures of dust ion acoustic waves in nonextensive dusty plasmas. Eur. Phys. J. D **69**(9), 1–8 (2015)
16. S. Das, Propagation of dust ion acoustic solitary waves in dusty plasma with Boltzmann electrons. J. Phys.: Conf. Ser. **1290**(1), 012025 (2019)
17. N.R. Kundu, M.M. Masud, K.S. Ashrafi, A.A. Mamun, Dust-ion-acoustic solitary waves and their multi-dimensional instability in a magnetized nonthermal dusty electronegative plasma. Astrophys. Space Sci. **343**(1), 279–287 (2013)
18. Y. Nakamura, A. Sarma, Observation of ion-acoustic solitary waves in a dusty plasma. Phys. Plasmas **8**(9), 3921–3926 (2001)
19. M.M. Masud, A.A. Mamun, Obliquely propagating dust-acoustic solitary waves in magnetized dusty plasmas with two-temperature Maxwellian ions. JETP Lett. **96**(12), 765–768 (2013)
20. U. Kumar Samanta, A. Saha, P. Chatterjee, Bifurcations of dust ion acoustic travelling waves in a magnetized dusty plasma with aq-nonextensive electron velocity distribution. Phys. Plasmas **20**(2), 022111 (2013)
21. A.A. Mamun, A. Mannan, Solitary waves and double layers in complex plasma media, Waves in Random and Complex Media, 1–12 (2021)
22. A.A. Mamun, R.A. Cairns, P.K. Shukla, Effects of vortex-like and non-thermal ion distributions on non-linear dust-acoustic waves. Phys. Plasmas **3**(7), 2610–2614 (1996)
23. C.-R. Choi, D.-Y. Lee, Y.-H. Kim, N.C. Lee, Effects of charged dust particles on nonlinear ion acoustic solitary waves in a relativistic plasma. Phys. Plasmas **16**(4), 043701 (2009)
24. H.F. Liu, S.Q. Wang, C.Z. Li, Q. Xiang, F.Z. Yang, Y. Liu, Cylindrical and spherical dust-ion acoustic solitary waves in a relativistic dust plasma. Phys. Scr. **82**(6), 065402 (2010)
25. B.C. Kalita, S. Das, Weakly Relativistic Ion-Acoustic Solitary Waves in Dusty Plasma. IEEE Trans. Plasma Sci. **46**(4), 790–796 (2017)
26. H.F. Liu, S.Q. Wang, Z. Wang, F.Z. Yang, Y. Liu, S. Li, Propagation of cylindrical and spherical dust-ion acoustic solitary waves in a relativistic dusty plasma. Adv. Space Res. **51**(12), 2368–2373 (2013)
27. B. Sahu, R. Roychoudhury, Electron-acoustic solitary waves and double layers in a relativistic electron-beam plasma system. Phys. Plasmas **11**(5), 1947–1954 (2004)
28. F. Verheest, S.R. Pillay, Large amplitude dust-acoustic solitary waves and double layers in nonthermal plasmas. Phys. Plasmas **15**(1), 013703 (2008)
29. R. Saeed, A. Shah, M. Noaman-ul-Haq, Nonlinear Korteweg-de Vries equation for soliton propagation in relativistic electron-positron-ion plasma with thermal ions. Phys. Plasmas **17**(10), 102301 (2010)
30. H.R. Pakzad, Dust acoustic solitary waves in dusty plasma with nonthermal ions. Astrophys. Space Sci. **324**(1), 41–45 (2009)
31. N. N. Rao, P. K. Shukla, M. Y. YU, Dust-acoustic waves in dusty plasmas. Planet. Space Sci. **38**(4), 543–546 (1990)
32. X. Qi, Y. Xu, W. Duan, L. Yang, The application scope of the reductive perturbation method and the upper limit of the dust acoustic solitary waves in a dusty plasma. Phys. Plasmas **21**(1), 013702 (2014)
33. B.C. Kalita, S. Das, D. Bhattacharjee, Determination of the measure of size (amplitude) of perturbation and its role in the process of enforcing discrete Korteweg-de Vries solitons to modified Korteweg-de Vries solitons as means of continuum hypothesis in a multi-component dusty plasma. Phys. Plasmas **24**(10), 102121 (2017)
34. F. Verheest, C.P. Olivier, W.A. Hereman, Modified Korteweg-de Vries solitons at supercritical densities in two-electron temperature plasmas. J. Plasma Phys. **82**(2), 1 (2016)
35. M. Wadati, The exact solution of the modified Korteweg-de Vries equation. J. Phys. Soc. Jpn. **32**(6), 1681 (1972)
36. F. Verheest, *Waves in Dusty Space Plasmas*, Vol. **245**, pp. 109–116 (Springer, 2000)
37. R.C. Davidson, *Methods in Nonlinear Plasma Theory* (Academic Press, 1972)